JOURNAL OF NATURAL PRODUCTS

ARTICLE

pubs.acs.org/jnp

Chaxamycins A−D, Bioactive Ansamycins from a Hyper-arid Desert *Streptomyces* sp.

Mostafa E. Rateb,[†,‡] Wael E. Houssen,[†,§] Markus Arnold,[§] Mostafa H. Abdelrahman,[†] Hai Deng,[†] William T. A. Harrison,[†] Chinyere K. Okoro,[⊥] Juan A. Asenjo,[∥] Barbara A. Andrews,[∥] Gail Ferguson,[§] Alan T. Bull,[#] Michael Goodfellow,[⊥] Rainer Ebel,[†] and Marcel Jaspars*[,†]

[†]Marine Biodiscovery Centre, Department of Chemistry, University of Aberdeen, Meston Walk, Aberdeen AB24 3UE, Scotland, U.K.

[‡]Pharmacognosy Department, Faculty of Pharmacy, Beni-Suef University, Salah Salem Street, Beni-Suef 32514, Egypt

[§]Institute of Medical Sciences, School of Medicine and Dentistry, University of Aberdeen, Ashgrove Road West, Aberdeen AB25 2ZD, Scotland, U.K.

[⊥]School of Biology, University of Newcastle, Newcastle upon Tyne NE1 7RU, U.K.

[∥]Centre for Biochemical Engineering and Biotechnology, Institute for Cell Dynamics and Biotechnology; a Centre for Systems Biology, University of Chile, Beauchef 850, Santiago, Chile

[#]School of Biosciences, University of Kent, Canterbury, Kent CT2 7NJ, U.K.

Supporting Information

ABSTRACT: *Streptomyces* sp. strain C34, isolated from soil collected in the Chilean hyper-arid Atacama Desert, was cultured on different media, resulting in the isolation and identification of four new ansamycin-type polyketides. The organism was selected for chemical investigation on the basis of a genome-mining PCR-based experiment targeting the gene encoding rifamycin-specific 3-amino-5-hydroxybenzoic acid synthetase (AHBA). The isolated compounds were structurally characterized using NMR and MS techniques and named chaxamycins A−D (**1**−**4**). Compounds **1**−**4** were tested for their antibacterial activity against *Staphylococcus aureus* ATCC 25923 and *Escherichia coli* ATCC 25922 and for their ability to inhibit the intrinsic ATPase activity of the heat shock protein 90 (Hsp90). Chaxamycin D (**4**), which showed a selective antibacterial activity against *S. aureus* ATCC 25923, was tested further against a panel of MRSA clinical isolates. In a virtual screening experiment, chaxamycins A−D (**1**−**4**) have also been docked into the ATP-binding pocket in the N-terminal domain of the Hsp90, and the observed interactions are discussed.

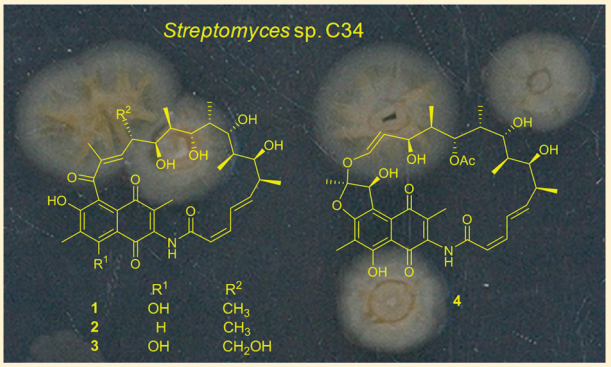

Microbial natural products form a mainstay of the drug-discovery industry due to their structural diversity and biological activity. More than 22 000 microbial secondary metabolites have been described up to 2009.[1] Filamentous bacteria belonging to the order Actinomycetales, especially the genus *Streptomyces*, have a proven capacity to produce novel bioactive secondary metabolites.[2−4] Recently, a higher rate of reisolation of known compounds from previously studied actinomycetes has been observed, thereby emphasizing the need to isolate, characterize, and screen representatives of novel actinomycete taxa.[5] It has also become clear that unusual and underexplored habitats, such as desert biomes and marine ecosystems, are a rich source of novel actinomycetes with the capacity to produce interesting new bioactive compounds.[6,7] One of the least explored habitats is the Atacama Desert in northern Chile. It is known to be the driest desert on Earth, where conditions have been considered too extreme for any sort of life to survive, with high levels of UV radiation, the presence of inorganic oxidants, areas of high salinity, and very low concentrations of organic carbon. Despite such adversity, novel actinomycetes have been isolated and identified from this hyper-arid environment.[8]

We have had the opportunity to investigate a total of 21 *Streptomyces* strains isolated from sediments collected from Laguna de Chaxa, Salar de Atacama, Chile. A molecular PCR-based approach was used to scan the genomes of these strains for interesting biosynthetic loci and thus to prioritize the samples for chemical investigation. Molecular-based approaches are essential to fully harness the biosynthetic capacity of these organisms that may be cryptic under any specific laboratory culture conditions. 3-Amino-5-hydroxybenzoic acid (AHBA) is the precursor of many natural products, such as mycotrienine,[9] ansamitocin

Received: April 14, 2011
Published: May 09, 2011

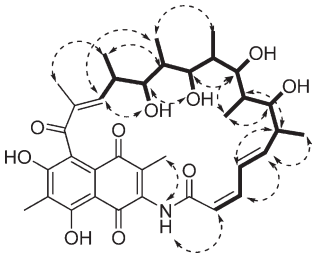

Figure 1. Key COSY (—) and ROESY (↔) correlations of **1**.

P-3,[10] and geldanamycin,[11] and the clinically used drugs rifamycin[12] and mitomycin C.[13] AHBA synthase is a key enzyme that catalyzes the last reaction in AHBA biosynthesis, the aromatization of 5-deoxy-5-aminodehydroshikimic acid. Therefore, the AHBA synthase gene can serve as a useful tool in the genetic screening for diverse AHBA-derived new natural products.[14] Chemical investigation of one of these novel strains guided by the PCR results revealed the characterization of four new ansamycin-type polyketides.

Structurally, ansamycins are characterized by a macrocycle composed of a benzenic or naphthalenic chromophore bridged by an aliphatic ansa chain that terminates at the chromophore in an amide linkage.[15] It is interesting to note that ansamycins are related structurally to maytansine and other maytansinoids obtained from plants of the genera *Maytenus* and *Putterlickia*.[16] Recent evidence supports the hypothesis that these plant compounds are biosynthesized by commensal actinomycetes.[17]

Ansamycins show antimicrobial activity against many Gram-positive and some Gram-negative bacteria. Also, these compounds show antiviral activity toward bacteriophages and poxviruses.[18] In addition, the ansamycin class of natural products is well known for its antitumor effects through the selective interaction with the ATP-binding pocket in the N-terminal domain of the heat shock protein 90 (Hsp90).[19] Hsp90 is involved in ensuring adequate cellular protein folding and preventing nonspecific aggregation of proteins following chemical mutation or stress.[20] Inhibition of Hsp90 leads to selective degradation of important proteins involved in cell proliferation, cell cycle regulation, and apoptosis, processes that are fundamentally important in the development of cancer.[21] Many examples are reported of this chemical scaffold including geldanamycin, a benzenoid ansamycin, first isolated from the culture filtrate of *Streptomyces hygroscopicus*,[22] and its semisynthetic derivative, 17-allylamino-17-demethoxygeldanamycin (17-AAG) or tanespimycin, which is currently in phase I clinical trials.[23]

The isolated compounds were tested for their antibacterial activity as well as for their ability to inhibit the intrinsic ATPase activity of the molecular chaperone Hsp90 using the colorimetric malachite green assay.[24] Compounds **1**−**4** were also docked into the ATP-binding pocket in the N-terminal domain of Hsp90, and the observed interactions are discussed.

RESULTS AND DISCUSSION

Among a total of 21 strains, only one, *Streptomyces* sp. C34, gave rise to a PCR product of the expected size of 760 bp, showing 73% GC content. Upon alignment, the deduced amino acid sequence displayed 87% identity to other AHBA synthases (Figure 1, Supporting Information).

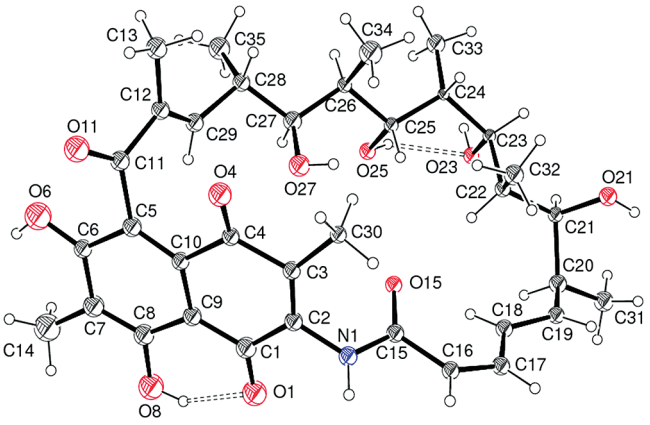

Figure 2. Molecular structure of **1** showing 30% displacement ellipsoids for the non-hydrogen atoms and intramolecular O−H···O hydrogen bonds as double-dashed lines. In the crystal structure, each organic molecule is accompanied by four-and-a-half water molecules of crystallization (not shown).

Subsequent chemical investigation of *Streptomyces* sp. C34 grown on ISP2 and modified ISP2 media, containing glycerol instead of glucose, revealed four new ansamycin-type polyketides (**1**−**4**). Interestingly, compounds **1** and **2** were isolated from ISP2 medium,[25] while compounds **1**, **3**, and **4** were obtained from the modified ISP2 (Figure 2, Supporting Information).

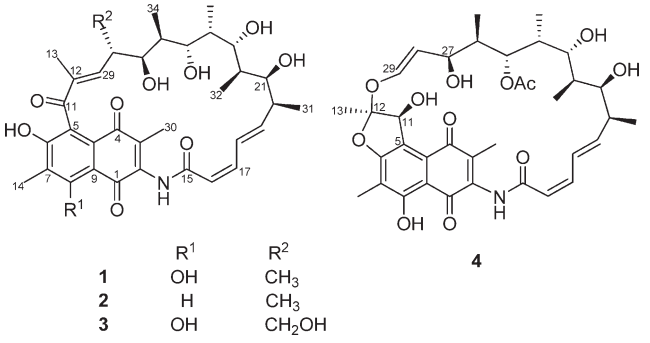

	R^1	R^2
1	OH	CH_3
2	H	CH_3
3	OH	CH_2OH

4

The ^{13}C NMR data and HRESIMS analysis of **1** indicated the molecular formula $C_{35}H_{45}NO_{10}$, and thus 14 degrees of unsaturation. The UV spectrum (MeOH) of **1** showed characteristic absorption maxima at 246, 270, 312, 338 (sh), and 393 nm, suggesting a naphthoquinone nucleus as a chromophore.[26] The ^{13}C NMR spectroscopic data of **1** (Table 1) showed two carbonyl signals at δ_C 185.2 and 183.7, characteristic for the quinone carbonyls,[26] one signal consistent with an α,β-unsaturated ketone at δ_C 196.3, and one amide carbon at δ_C 163.6. It also showed four oxygenated carbons at δ_C 65−80 as well as eight methyl carbons at δ_C 8−20. The ^1H NMR data (Table 1) revealed the presence of two olefinic and one aromatic methyl singlet (δ_H 1.90, 1.74, and 2.14, respectively), four hydroxy groups at δ_H 4−5, a set of four conjugated diene protons [δ_H 6.03 (d, 10.8 Hz), 6.66 (t, 11.0 Hz), 7.73 (dd, 11.1, 16.0 Hz), and 6.12 (dd, 6.4, 16.0 Hz)], and an olefinic proton [δ_H 6.35 (d, 6.8 Hz)] as well as an amide NH at δ_H 9.91 (s). This analysis brought the total number of unsaturations to 13, and thus, one more ring had to be incorporated into the structure of **1**.

In the COSY spectrum of **1**, a contiguous spin system was revealed comprising H-16 through H-29 and the methyl or

dx.doi.org/10.1021/np200320u |*J. Nat. Prod.* 2011, 74, 1491–1499

Table 1. NMR Spectroscopic Data (400 MHz, DMSO-d_6, 298 K) for Chaxamycins A (1) and B (2)

	chaxamycin A (**1**)			chaxamycin B (**2**)		
position	δ_C (mult.)	δ_H (mult., J Hz)	HMBC[a]	δ_C (mult.)	δ_H (mult., J Hz)	HMBC[a]
1	185.2, C			180.7, C		
2	138.2, C			138.3, C		
3	138.6, C			137.4, C		
4	183.7, C			184.4, C		
5	124.4, C			128.2, C		
6	159.3, C			157.5, C		
7	117.3, C			131.2, C		
8	161.1, C			129.2, CH	7.83 (s)	1, 6, 7, 14
9	106.5, C			122.7, C		
10	128.6, C			130.1, C		
11	196.3, C			196.6, C		
12	135.7, C			135.7, C		
13	11.8, CH_3	1.90 (s)	11, 12, 29	11.7, CH_3	1.92 (s)	11, 12, 29
14	8.7, CH_3	2.14 (s)	6, 7, 8	16.9, CH_3	2.34 (s)	6, 7, 8
15	163.6, C			163.6, C		
16	118.8, CH	6.03 (d, 10.8)	15, 18	119.0, CH	6.04 (d, 10.8)	15, 18
17	142.6, CH	6.66 (t, 11.0)	15, 19	142.4, CH	6.65 (t, 11.0)	15, 19
18	126.4, CH	7.73 (dd, 16.0, 11.0)	16, 17, 20	126.4, CH	7.73 (dd, 16.2, 11.2)	20
19	145.1, CH	6.12 (dd, 16.0, 6.4)	17, 20, 21, 31	144.9, CH	6.13 (dd, 16.0, 6.3)	17, 20, 21, 31
20	39.3, CH	2.25 (m)	18, 19, 21, 31	39.0, CH	2.27 (m)	21, 31
21	72.6, CH	4.03 (d, 7.3)	19, 20, 23, 32	72.6, CH	4.02 (d, 7.6)	31
22	33.7, CH	1.75 (m)	32	33.5, CH	1.73 (m)	
23	77.5, CH	3.34 (dd, 8.7, 3.8)	21	77.4, CH	3.33 (dd, 8.5, 3.2)	21
24	35.7, CH	1.73 (m)	23, 33	35.7, CH	1.72 (m)	23
25	68.9, CH	3.79 (d, 10.1)	27, 33, 34	68.9, CH	3.77 (d, 9.9)	34
26	42.4, CH	1.24 (m)	27, 34	42.2, CH	1.24 (m)	34
27	71.7, CH	3.82 (br s)	25, 28, 29, 34, 35	71.6, CH	3.82 (br s)	29, 34, 35
28	38.7, CH	2.43 (m)	12, 29, 35	38.9, CH	2.43 (m)	35
29	144.5, CH	6.35 (d, 8.5)	11, 13, 27, 28, 35	145.1, CH	6.31 (d, 8.5)	11, 13, 27
30	13.8, CH_3	1.74 (s)	2, 3, 4	13.9, CH_3	1.74 (s)	2, 3, 4
31	17.5, CH_3	0.86 (d, 6.8)	19, 20, 21	17.6, CH_3	0.86 (d, 7.0)	19, 20, 21
32	11.3, CH_3	0.88 (d, 6.8)	21, 22, 23	11.3, CH_3	0.88 (d, 7.0)	21, 22, 23
33	8.9, CH_3	0.64 (d, 6.7)	23, 24, 25	8.9, CH_3	0.63 (d, 6.6)	23, 24, 25
34	8.5, CH_3	0.27 (d, 6.9)	25, 26, 27	8.6, CH_3	0.25 (d, 6.8)	25, 26, 27
35	19.2, CH_3	0.92 (d, 7.0)	27, 28, 29	19.2, CH_3	0.93 (d, 7.0)	27, 28, 29
NH		9.91 (s)	1, 2, 3, 15		9.87 (s)	2, 3, 15
OH-21		4.34 (br s)	20, 21		4.34 (d, 2.5)	20
OH-23		4.84 (d, 6.5)	22, 23, 24		4.80 (d, 6.7)	22, 23
OH-25		3.83 (br s)	26		3.81 (br s)	
OH-27		4.08 (d, 5.0)	26, 28		4.08 (d, 5.1)	

[a] HMBC correlations, optimized for 8 Hz, are from the proton(s) stated to the indicated carbon(s).

hydroxy protons connected to this chain (Figure 1). These COSY correlations led to the establishment of a typical 14-carbon-substituted ansa chain, for which the connection to the rest of the structure was confirmed by HMBC correlations of H_3-13 to C-11, C-12, and C-29 and of H-17 to C-15. The presence of the naphthoquinone moiety was corroborated through the HMBC correlations of H_3-30 to C-2, C-3, and C-4 as well as H_3-14 to C-6, C-7, and C-8. The connection of the amide NH to the C-2 of the naphthoquinone moiety was confirmed by its HMBC correlations to C-1, C-2, and C-3. Finally, to account for the remaining degree of unsaturation, the ansa chain was judged to be connected to C-5 of the naphthoquinone system via C-11. On the basis of this data, the planar structure of **1** was established.

Owing to the difficulty of assigning the relative stereochemistry of this compound due to the conformational freedom of the ansa chain, the relative configuration of **1** was derived by the analysis of its crystal structure using single-crystal X-ray diffraction. The stereochemistry of the double bonds was established as *Z* at C-16−C-17 and *E* at C-18−C-19, C-12−C-29, and C-2−C-3, while the C-16−C-17−C-18−C-19 torsion angle was 166.8 (16)°, indicating the conformation of the C-17−C-18 bond to be

dx.doi.org/10.1021/np200320u |*J. Nat. Prod.* 2011, 74, 1491–1499

Table 2. Torsion Angles (deg) in the Aliphatic Chain in 1

C20−C21−C22−C23	−139.1 (13)
C21−C22−C23−C24	−167.5 (12)
C22−C23−C24−C25	−52.8 (16)
C23−C24−C25−C26	177.7 (11)
C24−C25−C26−C27	−178.8 (12)
C25−C26−C27−C28	−173.3 (13)
C26−C27−C28−C29	−167.3 (13)
C27−C28−C29−C12	137.5 (17)

s-trans (Figure 2). The relative configurations of the nine adjacent stereogenic centers in the aliphatic chain were identified as C-20 *S**, C-21 *S**, C-22 *R**, C-23 *R**, C-24 *R**, C-25 *R**, C-26 *R**, C-27 *S**, and C-28 *S**. The C-1−C-2−N-1−C-15 and the C-6−C-5−C-11−O-11 torsion angles were 116.2 (18)° and 65 (2)°, respectively, indicating that both the C-15 amide group and the C-11 ketone function were substantially twisted away from the plane of the naphthoquinone ring. A comparison of torsion angles along the aliphatic chain (C-20−C-29) (Table 2) revealed that five of the C−C−C−C bond conformations were approximately *anti* (*a*) and three (those about C-21−C-22, C-23−C-24, and C-28−C-29) were approximately *gauche* (*g*). The sequence along the chain was *gagaaaag*. On the basis of the riding model employed for the H atoms, two intramolecular O−H···O hydrogen bonds were judged to occur in **1**, between O-8−H-8···O-1 and O-25−H-25a···O-23. The other −OH groups and the N−H group formed hydrogen bonds to water molecules of crystallization.

As a reference for the assignments of the relative configuration of the other related compounds, a ROESY spectrum was measured, providing further support for the relative configuration of the stereogenic centers of the ansa chain and the geometry of the double bonds at C-2−C-3 and at C-12−C-29 (Figure 1), while the geometry of the double bonds at C-16−C-17 and C-18−C-19 was confirmed by ROESY and analysis of the coupling constants. Thus, **1** was identified as a new ansamycin-type polyketide, for which we propose the name chaxamycin A.

The ^{13}C NMR data and HRESIMS analysis of **2** revealed a molecular formula of $C_{35}H_{45}NO_9$, differing by loss of one oxygen atom relative to **1**. The comparison of the ^{1}H and ^{13}C NMR data of **2** (Table 1) with those of **1** indicated that **2** lacks a phenolic OH group at position 8 [δ_C 161.1 (C)], which was replaced by an aromatic proton [δ_C 129.2 (CH), δ_H 7.83 (s)]. HMBC correlations of H-8 to C-1, C-6, C-7, and C-14 and COSY and ROESY correlations of H-8 to H_3-14 were supportive of this conclusion. On the basis of the close similarity of the ^{13}C NMR data (Table 1) and similar ROESY correlations, it was confirmed that **2** has the same relative configuration as **1**. On this basis, **2** proved to be a new naturally occurring ansamycin, for which we propose the name chaxamycin B.

The ^{13}C NMR data and HRESIMS analysis of **3** indicated the molecular formula $C_{35}H_{45}NO_{11}$, revealing one more oxygen than **1**. The comparison of the ^{1}H and ^{13}C NMR spectra of **3** (Table 3) with those of **1** (Table 1) indicated that the methyl group at position 35 in **1** is hydroxylated in **3** [δ_C 62.0, δ_H 3.28 and 3.14]. The position of the hydroxymethyl group was confirmed by COSY correlations between H-28 and H_2-35 and by ROESY correlations between H_2-35 and H-29. The close similarity of the ^{13}C NMR data (Table 3) and the similar ROESY correlations confirmed that **3** has the same relative stereochemistry as **1**. Thus, **3** was identified as a new ansamycin-type congener, for which the name chaxamycin C is proposed.

The ^{13}C NMR data and HRESIMS analysis of **4** established its molecular formula as $C_{36}H_{45}NO_{12}$, thus containing one more carbon, two more oxygen atoms, and one additional degree of unsaturation in comparison to chaxamycin A (**1**). The similarity of its ^{1}H and ^{13}C NMR data (Table 3) to those of **1** indicated that both structures are related in the ansa chain and naphthoquinone ring. The 1D NMR spectra of **4** showed the lack of a signal for OH-25 and instead the appearance of an acetyl group [δ_C 171.0 (C-35), δ_C 20.8 (CH_3-36) and δ_H 1.97 (s)], which was found to be attached to C-25 on the basis of the HMBC correlations of both H-25 and H_3-36 to C-36. From the COSY spectrum, it was deduced that the fragment of the ansa chain comprising C-15 through C-27 was identical to that present in **1**, which was also supported by the HMBC spectrum (Table 3). The COSY correlation between H-27 and the deshielded H-28 [δ_C 118.5 (CH) and δ_H 5.00 (dd, J = 3.7, 12.1)] and between H-28 and H-29 indicated a new olefinic spin system.[27] The shielding of C-12 [δ_C 112.2 (C)] suggested the appearance of an acetal group substituted with a methyl group, H_3-13. HMBC correlations from H_3-13 to C-12 and C-11 confirmed this connectivity. The appearance of a new doublet in the ^{1}H NMR spectrum at δ_H 5.44 [δ_C 75.3, δ_H 5.44 (d, J = 4.9 Hz)] indicated the presence of a secondary alcohol moiety at C-11 instead of the ketone in **1**. This analysis accounted for 13 out of 15 degrees of unsaturation, thus requiring two additional rings in the structure. On the basis of NMR comparison with the literature and the HMBC correlations of H-11 to C-5, C-6, and C-10 and OH-11 (δ_H 5.54, d, J = 5.0 Hz) to C-5 and C-12, a hydroxyfuran ring condensed to the naphthoquinone system was established.[27] This 11-hydroxy-12-methyl-11-hydronaphtho[12,11-*b*]furan-1,4-dione substructure has been reported previously for the semisynthetic compounds rifabutinol[27] and rifamycinol.[28] To the best of our knowledge, this has not been encountered in nature so far. Finally, the HMBC correlation of H-29 to C-12 closed the ring at the ansa chain with the hydroxyfuran ring. This analysis confirmed that **4** is a new natural product of the rifamycin-type polyketides, for which we propose the name chaxamycin D.

The close similarity of the ^{13}C NMR (Table 3) and ROESY data indicated that **4** has the same relative stereochemistry as **1** in the ansa chain and naphthoquinone nucleus. The matching of NMR data and the coupling constant J_{28-29} with the value of 12.2 Hz, probably due to the effect of the neighboring electron-withdrawing group, as well as the X-ray analysis of similar compounds in literature, indicated an *E* configuration at C-28−C-29.[27−29] The close similarity of the NMR data for positions C-11 and C-12 with the previously described rifamycinol and rifabutinol[27−29] as well as the ROESY correlation between H-11 and H_3-13 indicated the relative configuration to be C-11 *R** and C-12 *S**.

A unique structural feature of the new ansamycins (**1**−**4**) that distinguishes them from the previously known members of this family is the lack of a methyl group at the olefinic C-16 next to the amide link when compared with previously isolated naphthalenic ansamycins such as the rifamycins, streptovaricins, tolypomycins, and halomicins, naphthomycin, actamycin, and damavaricins, and bransarols as well as benzenic ansamycins such as geldanamycin, and the herbimycins and macbecins.[18] Thus, chaxamycin A (**1**) is the 8-hydroxy-16-demethyl analogue of protostreptovaricin-I, and chaxamycin B (**2**) is the 16-demethyl analogue of protostreptovaricin-I.[30]

Table 3. NMR Spectroscopic Data (400 MHz, DMSO-d_6, 298 K) for Chaxamycins C (3) and D (4)

	chaxamycin C (3)			chaxamycin D (4)		
position	δ_C (mult.)[a]	δ_H (mult., J Hz)	HMBC[b]	δ_C (mult.)	δ_H (mult., J Hz)	HMBC[b]
1	184.9, C			184.7, C		
2	137.3, C			138.1, C		
3	138.7, C			139.6, C		
4	184.1, C			184.6, C		
5				124.0, C		
6	159.1, C			162.2, C		
7	116.2, C			111.7, C		
8	161.2, C			162.4, C		
9				108.3, C		
10				126.5, C		
11	197.1, C			75.3, CH	5.44 (d, 4.9)	5, 6, 10, 13
12	136.2, C			112.2, C		
13	11.9, CH_3	1.93 (s)	11, 12, 29	24.6, CH_3	1.77 (s)	11, 12
14	8.5, CH_3	2.07 (s)	6, 7, 8	8.0, CH_3	2.08 (s)	6, 7, 8
15	163.4, C			164.2, C		
16	118.8, CH	6.05 (d, 10.7)	15, 18	119.3, CH	6.00 (d, 10.9)	15, 18
17	142.5, CH	6.65 (t, 10.9)	15, 19	143.7, CH	6.61 (t, 11.1)	15, 19
18	126.3, CH	7.79 (dd, 16.1, 11.1)		125.8, CH	7.43 (m)	
19	144.8, CH	6.14 (dd, 16.1, 6.1)	17, 21	145.4, CH	6.19 (dd, 15.9, 6.2)	
20	38.7, CH	2.23 (m)	21, 31	38.1, CH	2.23 (m)	
21	72.2, CH	4.07 (d, 8.2)		72.6, CH	3.83 (m)	
22	32.9, CH	1.75 (m)		32.5, CH	1.70 (m)	
23	77.2, CH	3.44 (m)	21	76.4, CH	3.02 (m)	
24	35.9, CH	1.74 (m)		36.7, CH	1.73 (m)	
25	68.7, CH	3.81 (m)	33	74.0, CH	5.17 (dd, 9.9, 1.4)	23, 27, 33, 35
26	42.6, CH	1.21 (m)		38.4, CH	1.40 (m)	
27	66.6, CH	4.31 (d, 5.4)	29, 34	65.9, CH	3.86 (m)	
28	47.7, CH	2.36 (m)		118.5, CH	5.00 (dd, 12.2, 3.7)	27, 29
29	140.1, CH	6.26 (d, 8.5)		139.9, CH	5.96 (dd, 12.2, 1.6)	12, 27, 28
30	13.6, CH_3	1.73 (s)	2, 3, 4	12.9, CH_3	1.90 (s)	2, 3, 4
31	17.3, CH_3	0.84 (d, 6.7)	19, 20, 21	17.2, CH_3	0.81 (d, 7.0)	19, 20, 21
32	11.0, CH_3	0.90 (d, 6.9)	21, 22, 23	11.0, CH_3	0.90 (d, 6.9)	21, 22, 23
33	8.6, CH_3	0.61 (d, 6.7)	23, 24, 25	9.3, CH_3	0.64 (d, 6.7)	23, 24, 25
34	8.8, CH_3	0.26 (d, 6.9)	25, 26, 27	7.2, CH_3	0.05 (d, 6.7)	25, 26, 27
35	62.0, CH_2	3.28 (m)	27	171.0, C		
		3.14 (m)				
36				20.8, CH_3	1.97 (s)	35
NH		9.85 (s)	1, 2, 15		9.96 (s)	1, 2, 15
OH-8					12.76 (s)	7, 8, 9
OH-11					5.54 (d, 5.0)	5, 11, 12
OH-21		4.33 (d, 2.3)			4.33 (d, 1.9)	
OH-23		4.83 (d, 6.4)			4.77 (d, 5.9)	
OH-25		3.74 (d, 5.2)				
OH-27		4.03 (d, 5.3)			4.01 (d, 4.4)	

[a] Extracted from HSQC and HMBC spectra. [b] HMBC correlations, optimized for 8 Hz, are from the proton(s) stated to the indicated carbon(s).

Chaxamycins A–D (**1**–**4**) were tested for their antibacterial activity against the Gram-positive *S. aureus* ATCC 25923 and the Gram-negative *E. coli* ATCC 25922 (Table 4). Chaxamycin D (**4**), which showed a highly selective antibacterial activity against *S. aureus* ATCC 25923, has been tested further against a panel of clinical isolates of methicillin-sensitive as well as methicillin-resistant *S. aureus* (MRSA). Chaxamycin D (**4**) displayed activity against almost all strains, with MIC values less than 1 μg mL^{-1}, while rifampicin was distinctly more active, with MIC values ranging between 0.002 and 0.008 μg mL^{-1}, which was consistent with previous reports (Table 4).[31] Within the panel, only the epidemic EMRSA 16 strain proved quite resistant to both compound **4** and rifampicin, warranting further studies into the underlying mechanism of resistance.

dx.doi.org/10.1021/np200320u |*J. Nat. Prod.* 2011, 74, 1491–1499

Table 4. Antibacterial Activity of Chaxamycin D (4)

		minimal inhibitory concentration (μg mL^{-1})	
strain	source of isolate	**4**	rifampicin
E. coli ATCC 25922[a]	ATCC	1.21 (n = 2)	nd
S. aureus ATCC 25923[a]	ATCC	0.05 (n = 2)	nd
S. aureus RN4220[a]		0.06−0.13 (n = 4)	0.002−0.004 (n = 3)
SMRSA 106	nasal swab	0.25 (n = 3)	0.004 (n = 3)
SMRSA 124	open wound	0.13 − 0.25 (n = 3)	nd
SMRSA 116	knee abscess	0.13 − 0.25 (n = 4)	0.002−0.008 (n = 3)
EMRSA 15	urine infection	0.06 (n = 2)	0.002−0.004 (n = 3)
SMRSA 161 (PR161)	thigh abscess	0.13−0.25 (n = 3)	nd
SMRSA 126	nasal swab	0.13 (n = 2)	nd
SMRSA 153	arm cellulitis	0.25 (n = 2)	nd
SMRSA 105	toe wound	0.13 (n = 2)	0.002−0.008 (n = 3)
EMRSA 16	graft wound	>32 (n = 2)	4 (n = 1)
SMRSA 161 (PF161d)	buttock abscess	0.25 (n = 2)	nd

[a] Laboratory strain. All clinical isolates were obtained from the NHS Grampian Microbiology Diagnostic Laboratory (abbreviations: EMRSA = epidemic MRSA; SMRSA = Scottish MRSA, n = number of experiments; nd = not determined).

Table 5. Inhibition of the Intrinsic ATPase Activity of Human Hsp90α after Incubation with 100 μM of Each Compound

compound	% inhibition at 100 μM
1	46
2	45
3	41
4	15
17-AAG	84

Chaxamycins A−D (**1**−**4**) were also tested for inhibitory effects toward the intrinsic ATPase activity of the human Hsp90, a well-established mechanism of the antitumor effects of ansamycin-type compounds,[19] using the colorimetric malachite green assay.[24] Compounds **1**−**3** showed activity at 100 μM (Table 5) with percentages of inhibition ranging from 46% for compound **1** to 41% for compound **3**. Compound **4** was the least active in the assay, with only 15% observed reduction in activity. 17-AAG at 100 μM was used as a positive control and caused 84% inhibition in activity. The unexpected low potency of the standard reagent at this high concentration could be explained in view of the studies conducted by Kamal and colleagues,[32] which demonstrateed elegantly that Hsp90 derived from tumor cells has >100-fold higher affinity for 17-AAG than Hsp90 from normal cells. Hsp90 derived from tumor cells is present in multichaperone complexes with high ATPase activity and high affinity for ligands such as ATP and 17-AAG, whereas Hsp90 from normal tissues is in a latent, uncomplexed state with weak affinity. Chiosis et al.[33] presented an alternative hypothesis and stated that the high antitumor potency of 17-AAG, which cannot be correlated with its observed weak in vitro binding affinity to Hsp90, may be due to its tendency to accumulate in cells.

To correlate these bioassay results with the structure of these four ansamycin analogues and compare them to the standard 17-AAG, we conducted a docking study to explain the structure−activity relationship. All five compounds were docked into the ATP-binding pocket of human Hsp90. The absolute stereochemistry used for the minimized structures of **1**−**4** was that consistent with literature studies, as judged by optical rotation values. Docking of 17-AAG (Figure 3a,c) revealed a network of hydrogen bonds with residues Asn-51 and Lys-112, and three water molecules. Most of the van der Waals contacts were established with residues Asn-51, Ser-52, Ala-55, Asp-93, Met-98, Phe-138, and Thr-184. This compound gave the most negative docking score (−11.801), which indicates more favorable binding. Chaxamycin A (**1**) (Figure 3b,d), on the other hand, formed hydrogen bonds only with Thr-184 and three water molecules and showed a docking score of −10.946. The docking scores of compounds **2**, **3**, and **4** were −10.554, −9.960, and −8.870, respectively. A plot of the Hsp90 inhibition versus docking scores gave an excellent correlation (0.92, Figure 3, Supporting Information). It is therefore apparent that the major change from 17-AAG to **1** confers a major change in binding affinity that is reflected in the docking study. The loss of a OH group at C-8 changes the percentage affinity only slightly, and the docking score was only slightly reduced, indicating that this group is not important in the binding process. Hydroxylation at C-35 has a similarly small effect. The addition of an extra ring in **4** affects both the percentage inhibition and docking score significantly. On going from 17-AAG to **1**−**3** and then to **4**, the flexibility of the ansa chain is reduced by the addition of extra rings in the structure, and this appears to be the most significant factor in activity and binding.

EXPERIMENTAL SECTION

General Experimental Procedures. Optical rotations were recorded using a Perkin-Elmer 343 polarimeter. UV and IR spectra were measured on a Perkin-Elmer Lambda 25 UV/vis spectrometer and a Thermo Nicolet IR 100 FT/IR spectrometer, respectively. NMR data were acquired on a Varian Unity INOVA 400 MHz spectrometer. High-resolution mass spectrometric data were obtained using a Thermo Instruments MS system (LTQ XL/LTQ Orbitrap Discovery) coupled to a Thermo Instruments HPLC system (Accela PDA detector, Accela PDA autosampler, and Accela pump). The following conditions were used: capillary voltage 45 V, capillary temperature 260 °C, auxiliary gas flow rate 10−20 arbitrary units, sheath gas flow rate 40−50 arbitrary

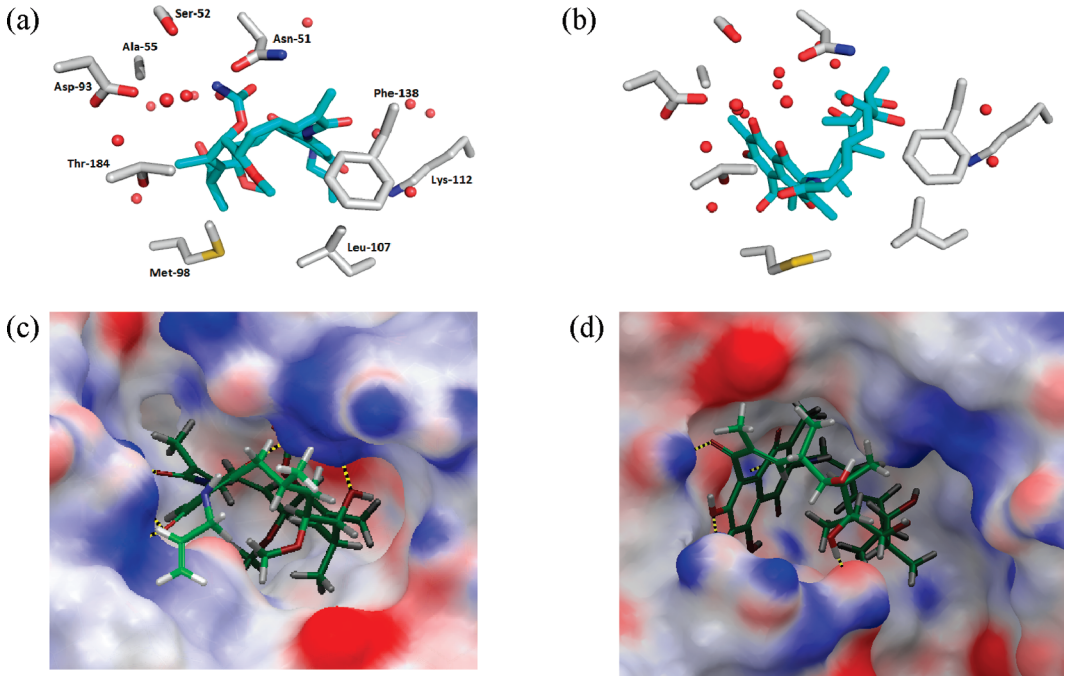

Figure 3. Binding of 17-AAG (left) and compound **1** (right) to the ATP-binding pocket in the N-terminal domain of human Hsp90α (PDB 1BYQ). The upper panel shows key protein residues and water molecules. Carbon atoms are in gray for the protein and in cyan for ligand. Oxygen, nitrogen, and sulfur atoms are red, blue, and yellow, respectively. The lower panel shows the electrostatic surface of the human Nt-Hsp90α (PDB 1BYQ) with 17-AAG (left) and compound **1** (right) docked into the ATP-binding pocket. Yellow dashed lines indicate hydrogen bonds between ligand and protein residues. Parts (a) and (b) are generated using PyMOL[34] (DeLano Scientific LCC).

units, spray voltage 4.5 kV, mass range 100−2000 amu (maximum resolution 30 000). HPLC separations were carried out using a Phenomenex reversed-phase (C_{18}, 250 × 10 mm, L × i.d.) column connected to an Agilent 1200 series binary pump and monitored using an Agilent photodiode array detector. Detection was carried out at 230, 254, 280, 360, and 410 nm. Malachite green, polyvinyl alcohol, and ATP sodium salt were obtained from Sigma-Aldrich. Ammonium molybdate was purchased from Lancaster Synthesis. Hsp90α protein was purchased from StressMarq Biosciences Inc. 17-AAG was obtained from Selleck Chemicals, Newmarket, UK. Diaion HP-20 was obtained from Resindion S.R.L., a subsidiary of Mitsubishi Chemical Co., Binasco, Italy.

Organism and Fermentation. Hyper-arid soil samples from the Laguna de Chaxa (Salar de Atacama, Chile) were collected aseptically by one of us (A.T.B.) in November 2004 and from which a collection of *Streptomyces* isolates were recovered.[8] A first-stage seed culture of *Streptomyces* sp. strain C34 (EU551711) was prepared by inoculating 50 mL of liquid medium with a single colony of the organism and incubating for 5 days at 28 °C with shaking at 150 rpm. The primary culture was used to inoculate a 3 L second stage culture that contained Diaion HP-20 (50 g L^{-1}). Incubation of the secondary culture was for 7 days at 28 °C with shaking at 150 rpm. Two different culture media were used: ISP2 medium[25] containing 4.0 g of yeast extract, 10.0 g of malt extract, 4.0 g of glucose, distilled water to 1 L, pH 7.20, and modified ISP2 medium containing 4.0 g of yeast extract, 10.0 g of malt extract, 10.0 g of glycerol, distilled water to 1 L, pH 7.20.

Genome Scanning. QIAprep Spin Miniprep kits (Qiagen) were used to prepare plasmids from *E. coli* strains. Wizard genomic DNA purification kits (Promega) were used to prepare genomic DNA from *Streptomyces* strain cultures grown on ISP2 medium. Restriction endonucleases, DNA ligase, DNA polymerase, and alkaline phosphatase were purchased from various sources and used according to the manufacturers' recommendations. DNA fragments were purified using Wizard PCR preps DNA purification system (Promega). PCR reactions were performed using AHBA-F (5′-TTC GAG CRS GAG TTC GC-3′) and AHBA-R (5′-GGA MCA TSG CCA TGT AG-3′) in 20 μL final volume with 5% DMSO and GoTaq DNA polymerase (1.5 U, Promega). PCR conditions were preheating at 98 °C for 5 min, followed by 30 cycles of denaturation at 95 °C for 30 s, annealing at 52 °C for 1 min, and extension at 72 °C for 40 s, with 7 min infilling at 72 °C. The PCR products were purified and ligated with pGEM-T easy vector for the blue−white screening. Plasmids were prepared from single colonies and sent for sequencing at the University of Dundee DNA sequencing facility (www.dnaseq.co.uk), accession number FR839674.

Extraction and Isolation. Culture broths were centrifuged (3000 rpm for 20 min), and the HP-20 resin together with the cell mass was washed with distilled water and extracted with methanol (5 × 500 mL). The successive MeOH extracts were combined and concentrated under reduced pressure to 250 mL and fractionated successively with *n*-hexane (3 × 250 mL), CH_2Cl_2 (3 × 250 mL), and EtOAc (3 × 250 mL). Quick NMR analysis revealed that the CH_2Cl_2 fraction had the most interesting metabolite profile. This fraction was loaded on a Sephadex LH-20 column equilibrated with MeOH−CH_2Cl_2 (1:1), and two fractions were collected. The second fraction (410 mg) was purified by semipreparative HPLC using a gradient of MeOH in H_2O (50−100% over 60 min) followed by 100% MeOH for 10 min at a flow rate of 1.25 mL/min to afford the pure compounds **1** (75 mg), **2** (28 mg), **3** (2 mg), and **4** (7 mg).

Chaxamycin A (***1***): yellow crystals (MeOH); mp 139.7 °C, $[\alpha]^{20}_{D}$ +157 (*c* 0.1, CH_3OH); UV (MeCN) λ_{max} (log ε) 246 (3.74), 270 (2.38), 312 (3.17), 338 (1.28, sh), 393 (2.97) nm; IR (film) ν_{max} 3478, 2937, 1728, 1539 cm^{-1}; ^1H and ^{13}C NMR, see Table 1; HRESIMS *m*/*z* 640.3116 $[M + H]^+$ (calcd for $C_{35}H_{46}NO_{10}$, 640.3122).

Chaxamycin B (***2***): yellow powder (MeOH); $[\alpha]^{20}_{D}$ +113 (*c* 0.1, CH_3OH); UV (MeCN) λ_{max} (log ε) 243 (3.71), 268 (2.39), 315 (3.15), 331 (1.27, sh), 385 (2.95) nm; IR (film) ν_{max} 3471, 2933, 1718,

1532 cm^{-1}; ^1H and ^{13}C NMR, see Table 1; HRESIMS m/z 624.3167 $[M + H]^+$ (calcd for $C_{35}H_{46}NO_9$, 624.3173).

*Chaxamycin C (**3**):* yellow powder (MeOH); $[\alpha]^{20}_D$ +117 (c 0.1, CH_3OH); UV (MeCN) λ_{max} (log ε) 247 (3.73), 271 (2.36), 313 (3.19), 335 (1.29, sh), 391 (2.98) nm; IR (film) ν_{max} 3476, 2935, 1721, 1537 cm^{-1}; ^1H and ^{13}C NMR, see Table 3; HRESIMS m/z 656.3065 $[M + H]^+$ (calcd for $C_{35}H_{46}NO_{11}$, 656.3071).

*Chaxamycin D (**4**):* yellow powder (MeOH); $[\alpha]^{20}_D$ +173 (c 0.1, CH_3OH); UV (MeCN) λ_{max} (log ε) 248 (3.84), 269 (2.45), 322 (3.14), 338 (1.28, sh), 387 (3.11), 412 (2.37) nm; IR (film) ν_{max} 3478, 2957, 1718, 1695, 1539 cm^{-1}; ^1H and ^{13}C NMR, see Table 3; HRESIMS m/z 706.2831 $[M + Na]^+$ (calcd for $C_{36}H_{45}NO_{12}Na$, 706.2839).

X-ray Crystallographic Study of 1. Intensity data for a weakly scattering yellow lath (0.20 × 0.05 × 0.04 mm) of $\mathbf{1}\cdot 4^1/_2\ H_2O$ were collected on a Nonius KappaCCD diffractometer (Mo Kα radiation, λ = 0.71073 Å) at T = 120 K. The structure was solved by direct methods with SHELXS-97 and the atomic model developed and refined against $|F^2|$ with SHELXL-97. Anisotropic refinement led to physically unrealistic ellipsoids, and all atoms were modeled with isotropic displacement parameters. Two of the water molecules must be partially occupied due to close intermolecular contacts, which results in $4^1/_2$ water molecules per organic molecule. The H atoms of the organic molecule were geometrically placed and refined as riding atoms; the −OH and $-CH_3$ moieties were refined as rotating rigid groups. The H atoms of the water molecules could not be unambiguously located either from difference maps or by geometrical placement, but a number of O···O contacts in the range 2.8−3.0 Å suggest the presence of O−H···O interactions in the crystal. The absolute structure was indeterminate in the present study, and Friedel pairs were merged before the final refinement. The highest difference peak is 0.62 Å from O1, and the deepest difference hole is 1.16 Å from H32a.

Crystal Data. $C_{35}H_{45}NO_{10}\cdot 4^1/_2H_2O$, M_r = 720.79, orthorhombic, $P2_12_12$ (No. 18), Z = 4, a = 24.5968(6) Å, b = 10.0636(2) Å, c = 14.6630(4) Å, V = 3629.57(15) $Å^3$, ρ = 1.319 g cm^{-3}, μ = 0.102 mm^{-1}, min., max. $\Delta\rho$ = −0.72, +0.83 e $Å^{-3}$, $R(F)$ = 0.199 [3438 reflections with $I > 2\sigma(I)$], $wR(F^2)$ = 0.410 (4000 reflections), S (goodness of fit) = 1.165. Crystallographic data (excluding structure factor tables) for the structures reported have been deposited with the Cambridge Crystallographic Data Center as supplementary publication no. CCDC 801850. Copies of the data can be obtained free of charge on application to CCDC, 12 Union Road, Cambridge CB 1EZ, UK [fax: Int.+44(0) (1223) 336 033); e-mail: deposit@ccdc.cam.ac.uk].

Antibacterial Screening. The antibacterial activity of compounds **1**−**4** was evaluated against both *S. aureus* ATCC 25923 and *E. coli* ATCC 25922 using an agar diffusion method and regression line analysis.[35] Filter paper disks containing oxolinic acid (2 μg) and ampicillin (10 μg) were used as positive controls. The activity of compound **4** was evaluated further on the methicillin-sensitive laboratory strain, *S. aureus* RN4220,[36] and a panel of methicillin-resistant *S. aureus* clinical isolates obtained from the NHS Grampian Microbiology Diagnostic Laboratory using slight modifications of the previously described method.[37] In brief, *S. aureus* strains were grown in Müller-Hinton (MH) broth[38] to early stationary phase and then diluted to an OD_{650} = 0.0005. The assays were performed in a 96-well microtiter plate format in triplicate, with at least two independent cultures for each strain. Rifampicin and compound **4** were dissolved in DMSO (Sigma), and the effect of different dilutions of both compounds (0.03−0.001 and 32−0.016 μg mL^{-1}, respectively) on the growth was assessed after 18 h incubation at 37 °C using a Labsystems iEMS Reader MF plate reader at OD_{620}. The MIC was determined as the lowest concentration showing no growth compared to the MH broth control. DMSO up to 0.63% was shown to have no antibacterial effect.

Hsp90 Assay. The ability of compounds **1**−**4** to inhibit the ATPase activity of the Hsp90 protein was evaluated and compared with that of the 17-AAG using the previously reported colorimetric malachite green assay.[24] The principle of the assay used is to determine the inorganic phosphate released after the hydrolysis of the ATP by purified Hsp90 using the reaction of the cationic dye malachite green with the phosphomolybdate complex to generate a blue-green color with an absorbance maximum at 610 nm.[39] The assay is complicated by the nonenzymatic hydrolysis of ATP mediated by molybdate that can be overcome by the addition of sodium citrate.[40] Compounds were tested in duplicate at a final concentration of 100 μM in 0.5% (v/v) DMSO. Background absorption due to chemical degradation of ATP was determined and subtracted from each reading. The assay was conducted in a flat-bottomed 96-well plate. All aqueous solutions were prepared with deionized water to minimize contamination by inorganic phosphate. Glassware and the pH meter were rinsed with double-distilled water before use. Plasticware was used wherever possible. Absorbance was read at 620 nm on a Labsystems iEMS Reader MF plate reader.

Docking Studies. Molecular modeling was conducted using the Schrodinger Suite 2010. Compounds **1**−**4**, ADP, and 17-AAG were submitted to a conformational search using Monte Carlo Multiple Minimum (MCMM) into MacroModel 9.8. The algorithm used was OPLS_2005 as the force field and a distance-dependent dielectric constant of 1.0. The crystal structure of the N-terminal domain of human Hsp90 in complex with ADP was retrieved from the Protein Data Bank (PDB entry 1BYQ).[41] Docking was performed with the Glide (Grid-based Ligand Docking with Energetics) program, version 5.6. The protein Preparation Wizard module of Maestro was used to prepare the protein. The compounds were then docked using the induced fit docking protocol[42] and the default parameters with the exception of selecting trim side chain during initial Glide docking and using XP (extra precision) scoring for the redock step.

■ ASSOCIATED CONTENT

Supporting Information. Sequence alignment of the PCR product amplified from the *Streptomyces* sp. C34 with other known genes encoding AHBA synthases, and NMR spectra of **1**−**4** including ^1H, ^{13}C, COSY, HSQC, HMBC, and ROESY in DMSO-d_6 are available free of charge via the Internet at http://pubs.acs.org.

■ AUTHOR INFORMATION

Corresponding Author

*Tel: +44 (0)1224 272895. Fax: +44 (0)1224 272921. E-mail: m.jaspars@abdn.ac.uk.

■ ACKNOWLEDGMENT

We thank DNA Sequencing & Services (MRCPPU, College of Life Sciences, University of Dundee, Scotland, www.dnaseq.co.uk) for DNA sequencing, A. Crossman, Department of Chemistry, University of Dundee, for determination of the optical activity, and the Egyptian Government for a Ph.D. scholarship to M.E.R. W.E.H. is the recipient of a SULSA postdoctoral fellowship. This work was supported in part by an MRC New Investigator grant (G0501107) awarded to G.P.F. M.A. is a SULSA-funded translational medicine Ph.D. student. We thank the College of Physical Sciences, University of Aberdeen, for provision of infrastructure and facilities in the Marine Biodiscovery Centre. A.T.B. thanks the Leverhulme Trust for an Emeritus Fellowship, and A.T.B. and J.A.S. thank the Royal Society for International Joint Project Grant JP100654. Financial support of

the Millenium Scientific Initiative (grant ICM-P05-001-F) is gratefully acknowledged.

REFERENCES

(1) Demain, A. L.; Sanchez, S. *J. Antibiot.* **2009**, *62*, 5–16.
(2) Bentley, S. D.; Chater, K. F.; Cerdeno-Tarraga, A. M.; Challis, G. L.; Thomson, N. R.; James, K. D.; Harris, D. E.; Quail, M. A.; Kieser, H.; Harper, D.; Bateman, A.; Brown, S.; Chandra, G.; Chen, C. W.; Collins, M.; Cronin, A.; Fraser, A.; Goble, A.; Hidalgo, J.; Hornsby, T.; Howarth, S.; Huang, C. H.; Kieser, T.; Larke, L.; Murphy, L.; Oliver, K.; O'Neil, S.; Rabbinowitsch, E.; Rajandream, M. A.; Rutherford, K.; Rutter, S.; Seeger, K.; Saunders, D.; Sharp, S.; Squares, R.; Squares, S.; Taylor, K.; Warren, T.; Wietzorrek, A.; Woodward, J.; Barrell, B. G.; Parkhill, J.; Hopwood, D. A. *Nature* **2002**, *417*, 141–147.
(3) Omura, S.; Ikeda, H.; Ishikawa, J.; Hanamoto, A.; Takahashi, C.; Shinose, M.; Takahashi, Y.; Horikawa, H.; Nakazawa, H.; Osonoe, T.; Kikuchi, H.; Shiba, T.; Sakaki, Y.; Hattori, M. *Proc. Natl. Acad. Sci. U. S. A.* **2001**, *98*, 12215–12220.
(4) Goodfellow, M.; Fiedler, H.-P. *Antonie van Leeuwenhoek* **2010**, *98*, 119–142.
(5) Hong, K.; Gao, A.-H.; Xie, Q.-Y.; Gao, H.; Zhuang, L.; Lin, H.-P.; Yu, H.-P.; Li, J.; Yao, Z.-S.; Goodfellow, M.; Ruan, J.-S. *Mar. Drugs* **2009**, *7*, 24–44.
(6) Bull, A. T.; Stach, J. E. *Trends Microbiol.* **2007**, *15*, 491–499.
(7) Bull, A. T. In *Extremophiles Handbook*; Horikoshi, K.; Antranikian, G.; Bull, A. T.; Robb, F. T.; Stetter, K. O., Eds.; Springer: New York, 2011; Vol. 2, Part 12, pp 1204−1240.
(8) Okoro, C. K.; Brown, R.; Jones, A. L.; Andrews, B. A.; Asenjo, J. A.; Goodfellow, M.; Bull, A. T. *Antonie van Leeuwenhoek* **2009**, *95*, 121–133.
(9) Chen, S.; von Bamberg, D.; Hale, V.; Breuer, M.; Hardt, B.; Muller, R.; Floss, H. G.; Reynolds, K. A.; Leistner, E. *Eur. J. Biochem.* **1999**, *261*, 98–107.
(10) Yu, T. W.; Bai, L. Q.; Clade, D.; Hoffmann, D.; Toelzer, S.; Trinh, K. Q.; Xu, J.; Moss, S. J.; Leistner, E.; Floss, H. G. *Proc. Natl. Acad. Sci. U. S. A.* **2002**, *99*, 7968–7973.
(11) Li, Y.; He, W.; Wang, Y.; Wang, Y.; Shao, R. *J. Antibiot.* **2008**, *61*, 347–355.
(12) Kim, C. G.; Kirschning, A.; Bergon, P.; Ahn, Y.; Wang, J. J.; Shibuya, M.; Floss, H. G. *J. Am. Chem. Soc.* **1992**, *114*, 4941–4943.
(13) Mao, Y.; Varoglu, M.; Sherman, D. H. *J. Bacteriol.* **1999**, *181*, 2199–2208.
(14) Huitu, Z.; Linzhuan, W.; Aiming, L.; Guizhi, S.; Feng, H.; Qiuping, L.; Yuzhen, W.; Huanzhang, X.; Qunjie, G.; Yiguang, W. *J. Appl. Microbiol.* **2009**, *106*, 755–763.
(15) Prelog, V.; Oppolzer, W. *Helv. Chim. Acta* **1973**, *56*, 2279–2287.
(16) Cassady, J. M.; Chan, K. K.; Floss, H. G.; Leistner, E. *Chem. Pharm. Bull.* **2004**, *52*, 1–26.
(17) Zhu, N.; Zhao, P.; Shen, Y. *Curr. Microbiol.* **2009**, *58*, 87–94.
(18) Wrona, I. E.; Agouridas, V.; Panek, J. S. *C. R. Chim.* **2008**, *11*, 1483–1522.
(19) Porter, J. R.; Ge, J.; Lee, J.; Normant, E.; West, K. *Curr. Top. Med. Chem.* **2009**, *9*, 1386–1418.
(20) Smith, D. F.; Whitesell, L.; Katsanis, E. *Pharmacol. Rev.* **1998**, *50*, 493–513.
(21) Hostein, I.; Robertson, D.; Di Stefano, F.; Workman, P.; Clarke, P. A. *Cancer Res.* **2001**, *61*, 4003–4009.
(22) DeBoer, C.; Meulman, P. A.; Wnuk, R. J.; Petreson, D. H. *J. Antibiot.* **1970**, *23*, 442–447.
(23) http://clinicaltrials.gov/ct2/results?term=17-AAG, accessed 10/04/2011.
(24) Rowlands, M. G.; Newbatt, Y. M.; Prodromou, C.; Pearl, L. H.; Workman, P.; Aherne, W. *Anal. Biochem.* **2004**, *327*, 176–183.
(25) Shirling, E. B.; Gottlieb, D. *Int. J. Syst. Bacteriol.* **1966**, *16*, 313–340.
(26) Cimino, G.; Coates, R. M.; De Stefano, S.; Fontana, A.; Hemmerich, P.; Minale, L.; Rinehart, K. L.; Shield, L. S.; Sodano, G.; Toniolo, C. *Fortschr. Chem. Org. Naturst.* **1976**, *33*, 231–307.
(27) Santos, L.; Medeiros, M. A.; Santos, S.; Costa, M. C.; Tavares, R.; Curto, M. J. M. *J. Mol. Struct.* **2001**, *563*−*564*, 61–78.
(28) Cellai, L.; Cerrini, S.; Lamba, D.; Brizzi, V.; Brufani, M. *J. Chem. Res. Synop.* **1987**, 328–329.
(29) Santos, L.; Fant, F.; Medeiros, M. A.; Borremans, F. A. M.; Costa, M. C.; Curto, M. J. M. *Magn. Reson. Chem.* **2000**, *38*, 937–945.
(30) Deshmukh, P. V.; Kakinuma, K.; Ameel, J. J.; Rinehart, K. L.; Wiley, P. F.; Li, L. H. *J. Am. Chem. Soc.* **1976**, *98*, 870–872.
(31) Zhao, X.; Drlica, K. *J. Infect. Dis.* **2002**, *185*, 561–565.
(32) Kamal, A.; Thao, L.; Sensintaffar, J.; Zhang, L.; Boehm, M. F.; Fritz, L. C.; Burrows, F. J. *Nature* **2003**, *425*, 407–410.
(33) Chiosis, G.; Huezo, H.; Rosen, N.; Mimnaugh, E.; Whitesell, L.; Neckers, L. *Mol. Cancer Ther.* **2003**, *2*, 123–129.
(34) DeLano, W. L. *The PyMOL Molecular Graphics System*; DeLano Scientific: Palo Alto, CA, USA, 2002; available at http://www.pymol.org.
(35) Kronvall, G. *J. Clin. Microbiol.* **1983**, *17*, 975–980.
(36) Rachid, S.; Ohlsen, K.; Wallner, U.; Hacker, J.; Hecker, M.; Ziebuhr., W. *J. Bacteriol.* **2000**, *182*, 6824–6826.
(37) Domenech, P.; Kobayashi, H.; LeVier, K.; Walker, G. C.; Barry, C. E. *J. Bacteriol.* **2009**, *191*, 477–485.
(38) Müller, H. J.; Hinton., J. *Proc. Soc. Exp. Biol. Med.* **1941**, *48*, 330–333.
(39) Baykov, A. A.; Evtushenko, O. A.; Avaeva, S. M. *Anal. Biochem.* **1988**, *171*, 266–270.
(40) Henkel, R. D.; Vandeberg, J. L.; Walsh, R. A. *Anal. Biochem.* **1988**, *169*, 312–318.
(41) Obermann, W. M. J.; Sondermann, H.; Russo, A. A.; Pavletich, N. P.; Hartl, F. U. *J. Cell Biol.* **1998**, *143*, 901–910.
(42) Sherman, W.; Day, T.; Jacobson, M. P.; Friesner, R. A.; Farid, R. *J. Med. Chem.* **2006**, *49*, 534–553.